Journal of Alloys and Compounds 506 (2010) 688–692

Contents lists available at ScienceDirect

Journal of Alloys and Compounds

journal homepage: www.elsevier.com/locate/jallcom

Effect of extrusion temperature on microstructures and damping capacities of Grp/AZ91 composite

Y.W. Wu*, K. Wu, K.K. Deng, K.B. Nie, X.J. Wang, X.S. Hu, M.Y. Zheng

School of Materials Science and Engineering, Harbin Institute of Technology, Harbin 150001, PR China

ARTICLE INFO

Article history:
Received 23 March 2010
Received in revised form 7 July 2010
Accepted 7 July 2010
Available online 15 July 2010

Keywords:
Magnesium matrix composite
Graphite particles
Extrusion
Damping capacities
Microstructures

ABSTRACT

Magnesium matrix composite reinforced by graphite particles was fabricated using stir casting with graphite particle size of 50 μm and graphite particle volume fraction of 10%. The as-cast composite was extruded at 250 °C, 300 °C and 350 °C with an extrusion ratio of 12:1. The experimental results reveal that the extrusion temperature plays an important role on the microstructures and damping capacities. The aspect ratio of graphite particles increases as the extrusion temperature rises. Extrusion at 300 °C leads to the highest damping values in low strain region at room temperature. It also demonstrates the highest damping values at elevated temperatures when the strain is 4×10^{-5}. In addition, there are two definite damping peaks in the damping-temperature curves which occur at about 150 °C and 350 °C, respectively.

1. Introduction

High damping and lightweight materials are drawing strong attention for engineering applications in various fields [1–3]. The damping capacities of a material refer to its ability to convert mechanical vibration energy into thermal energy or other energies. Materials that possess high damping capacities have several advantages, for example, eliminating unwanted noise and vibration, enhancing vehicle and instrument stability [4,5]. Lightweight systems, in which magnesium alloys are involved, are becoming more and more important in mechanical engineering such as robotics, machine-tools and automotive industry [6,7].

Magnesium matrix composites are good candidates for realizing high damping and lightweight. Magnesium alloys are widely employed in aerospace, electronics and automotive industry due to low density and high specific strength [8,9]. With the development of metal matrix composites technology, it becomes possible to further improve the damping capacities of magnesium alloys by adding high damping reinforcements. Magnesium alloys AZ series (Mg–Al–Zn) have been widely used in automobile industry encompassing parts such as steering wheels, steering column parts, instrument panels, seats, gear boxes, air intake system and so on, but their damping capacities are relatively low [10–12]. Graphite particles (Grp) are found to exhibit relatively high damping capacities when measured in its bulk form [13]. Therefore, the addition of graphite particles to magnesium alloy AZ91 (Mg–9 wt% Al–1 wt% Zn) will be quite promising in improving the damping capacities, and thus extend its application range. Hot extrusion is an increasingly attractive processing route to enhance mechanical properties including ductility and strength [14–17], but there has been no attempt made to study the effect of hot extrusion on damping capacities.

Accordingly, the primary aim of this paper was to study the effect of extrusion temperature on the damping capacities and microstructures of Grp/AZ91 composite, fabricated by stir casting. The relationship between damping capacities and microstructures was also discussed in light of the experimental results.

2. Experimental

A commercial magnesium alloy AZ91 was selected as the matrix, and flake graphite particles with an average size of 50 μm were employed as the reinforcement. The Grp/AZ91 composite with graphite particle volume fraction of 10% was fabricated by stir casting in a protective atmosphere of CO_2 and SF_6. The as-cast Grp/AZ91 composite was extruded at 250 °C, 300 °C and 350 °C with an extrusion ratio of 12:1 (marked as 250R12, 300R12 and 350R12) after T4 treatment (415 °C for 24 h), respectively.

The damping tests were carried out by dynamic mechanical analyzer (DMA) (Model TA Q800, USA) with single cantilever vibration mode. The damping capacities were determined by $Q^{-1} = \tan\phi$, where ϕ was the lag angle between the applied strain and the response stress. The dimensions of the damping test specimens were 35 mm × 8 mm × 1 mm. Measurements were made at various strain amplitudes (ε) from 5.3×10^{-6} to 1.3×10^{-3}, the vibration frequency (f) was 1 Hz, and the test temperature (T) was room temperature. For the measurements of temperature dependent damping capacities, the test conditions were as follows: the strain amplitude (ε) was 4×10^{-5}, the vibration frequency (f) was 1 Hz, the temper-

* Corresponding author at: 433# Harbin Institute of Technology, Harbin 150001, PR China. Tel.: +86 451 86402291; fax: +86 451 86413922.
E-mail address: wuyewei811105@yahoo.com.cn (Y.W. Wu).

0925-8388/$ – see front matter © 2010 Elsevier B.V. All rights reserved.
doi:10.1016/j.jallcom.2010.07.043

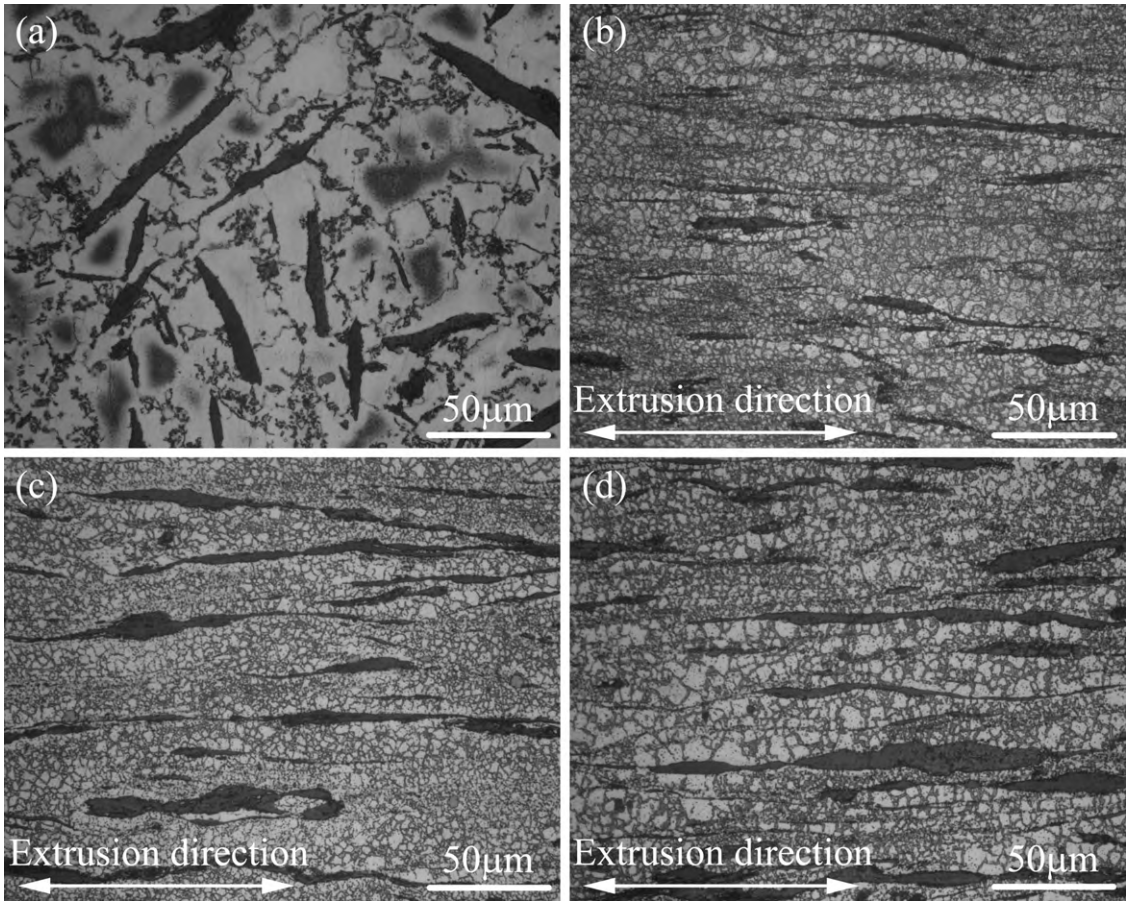

Fig. 1. Optical micrographs show grain size of composite in condition of: (a) as-cast; (b) 250R12; (c) 300R12; (d) 350R12.

ature range (T) was from room temperature to 400 °C and the heating rate ($\dot{T}$) was 5 °C/min.

The microstructures of Grp/AZ91 composite were examined under OLYMPUS-PMG3 type optical microscope (OM). In order to investigate the variation of grains and graphite particles during hot extrusion, the software Image-Pro Plus was used to analyse the images from OM.

3. Results and discussion

3.1. Microstructures of Grp/AZ91 composite

Figs. 1 and 2 show the optical micrographs of Grp/AZ91 composite. According to Fig. 1, the grain size is calculated by the software Image-Pro Plus, and the result is shown in Fig. 3. From Fig. 3, it can be seen that the grain size decreases significantly after hot extrusion, and extrusion at 250 °C leads to the finest grains. This is because relatively low extrusion temperature can effectively inhibit the growth of recrystallization grains. According to Fig. 2, the length, width and aspect ratio of graphite particles are calculated by the software Image-Pro Plus, and the results are shown in Figs. 4 and 5. The aspect ratio is the ratio between length and width, i.e. aspect ratio = length/width. It can be seen from Fig. 4 that hot extrusion increases the length of graphite particles, but decreases the width. Therefore, as shown in Fig. 5, hot extrusion can improve the aspect ratio of graphite particles, and the aspect ratio increases as the extrusion temperature rises. This indicates the aspect ratio of graphite particles is dependent on extrusion temperature. The increase of extrusion temperature can improve the mobility of matrix alloy, and thus increase the aspect ratio of graphite particles.

3.2. Damping capacities of Grp/AZ91 composite

Strain amplitude dependence of damping capacities in as-extruded Grp/AZ91 composite and AZ91 alloy are shown in Fig. 6. The curves can generally be divided into two parts, a strain independent part Q_0^{-1} at low strain and a strain dependent part Q_H^{-1} at high strain which increases with rising strain amplitude. Hence, the damping can be expressed by [18]:

$$Q^{-1}(\varepsilon) = Q_0^{-1} + Q_H^{-1}(\varepsilon) \tag{1}$$

It is noticeable that extrusion at 300 °C leads to the highest damping values in low strain region at room temperature. However, the damping values are very similar in relatively high strain region. This indicates the damping values are independent on extrusion temperature in relatively high strain region. From Fig. 6, it can be also seen that the damping capacities are improved significantly by the addition of graphite particles. When the composite and alloy are extruded at same temperature (300 °C), the Q_0^{-1} is 0.0059 for the composite and 0.0015 for the alloy, respectively. Compared with the alloy, the Q_0^{-1} of Grp/AZ91 composite is increased by nearly 400%.

The Q_H^{-1} is related to dislocations by the following equation derived from the Granato–Lücke (G–L) model [19,20]:

$$Q_H^{-1} = \frac{C_1}{\varepsilon} \exp\left(-\frac{C_2}{\varepsilon}\right) \tag{2}$$

$$C_1 = \frac{\rho F_B L_N^3}{6bEL_C^2} \tag{3}$$

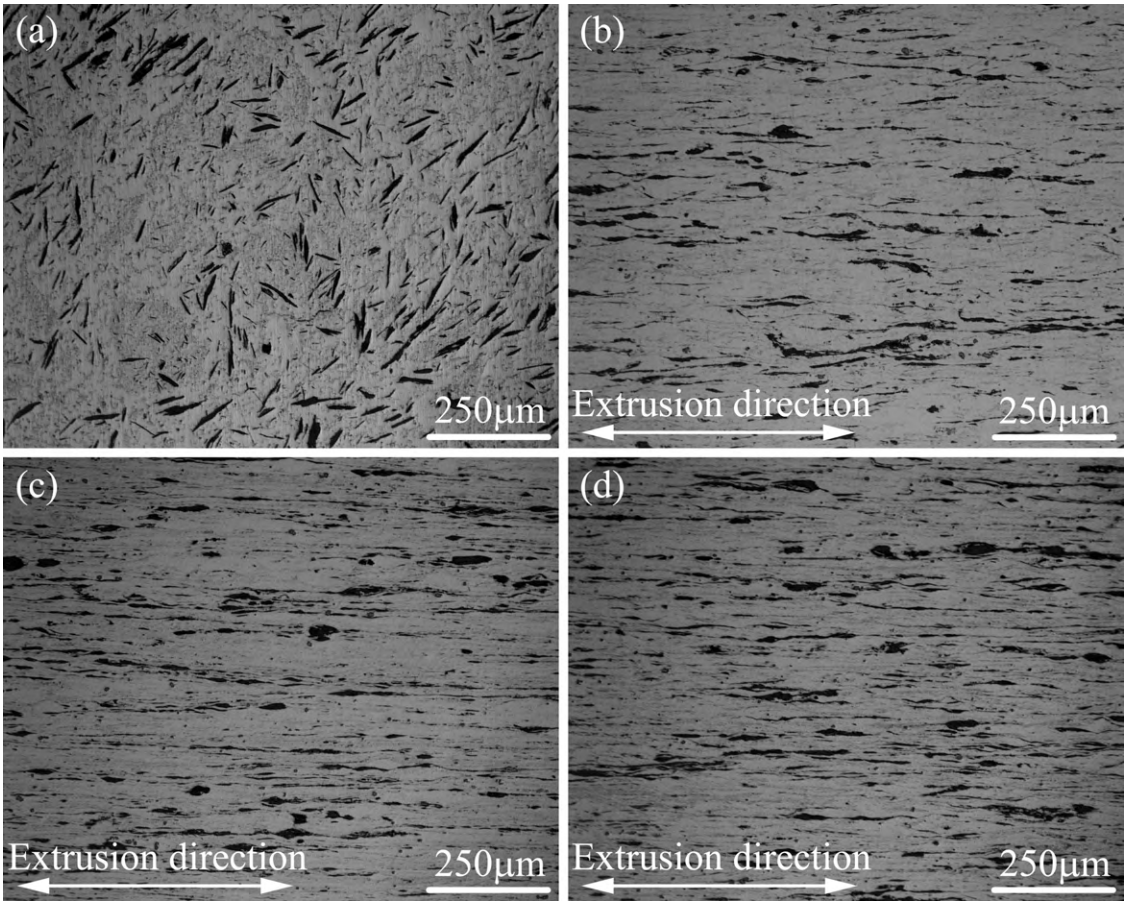

Fig. 2. Optical micrographs show particle distribution of composite in condition of: (a) as-cast; (b) 250R12; (c) 300R12; (d) 350R12.

$$C_2 = \frac{F_B}{bEL_C} \tag{4}$$

where ε is the strain amplitude; C_1 and C_2 are the material constants; ρ is the dislocation density; F_B is the binding force between dislocations and weak pinning points; E is the elastic modulus; L_C and L_N are the average dislocation distance between weak pinning points and strong pinning points, respectively; b is the Burger's vector. Eq. (2) can be alternated as:

$$\ln(Q_H^{-1}\varepsilon) = \ln\ C_1 - \frac{C_2}{\varepsilon} \tag{5}$$

It can be noted from Eq. (5) that the G–L plots should be straight lines, whose intercept and slope are the values of $\ln C_1$ and $-C_2$, respectively. From Fig. 7, it is shown that the as-extruded Grp/AZ91 composite follows the G–L model properly in relatively high strain region.

According to Granato–Lücke theory [19,20], matrix dislocations are pinned by the strong pinning points (such as network nodes of dislocations, grain boundaries, graphite particles, etc.) and the weak pinning points (such as solution atoms, vacancies, etc.). At low strain, dislocations can only drag the weak pinning points moving and thus dissipating energy. Hence, the damping from the dislocations is limited. With increasing strain, the stress increases. Above a certain strain, the unpinning of dislocations from the weak pinning points occurs in the snowslide-like mode. Dislocation string becomes long and comparatively free between strong pinning points. Thus the damping from the dislocations increases significantly. And then the energy dissipated by dislocation motion would not increase.

Therefore, in as-extruded Grp/AZ91 composite, the possible dominant damping mechanisms in relatively low strain region are intrinsic damping of graphite particles, particles/matrix interface damping, and grain boundary damping; while in relatively high strain region, matrix dislocation damping is likely to be responsible for a large portion of the observed damping.

Temperature dependence of damping capacities in as-extruded Grp/AZ91 composite are shown in Fig. 8. The damping capacities of as-extruded Grp/AZ91 composite are intensively dependent on

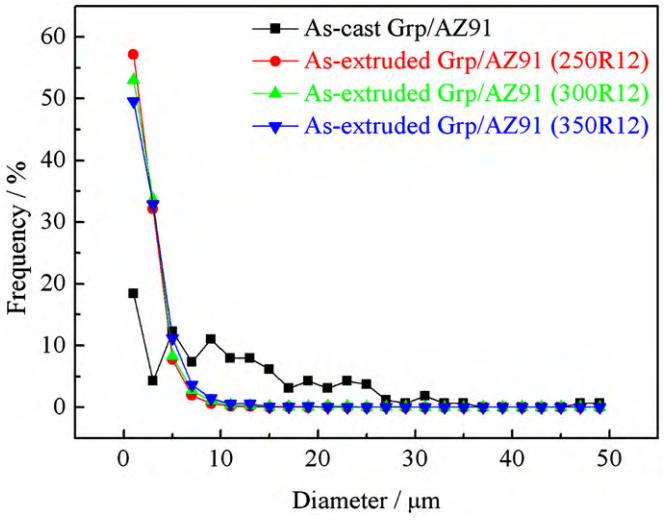

Fig. 3. Distribution of grain size of Grp/AZ91 composite before and after hot extrusion.

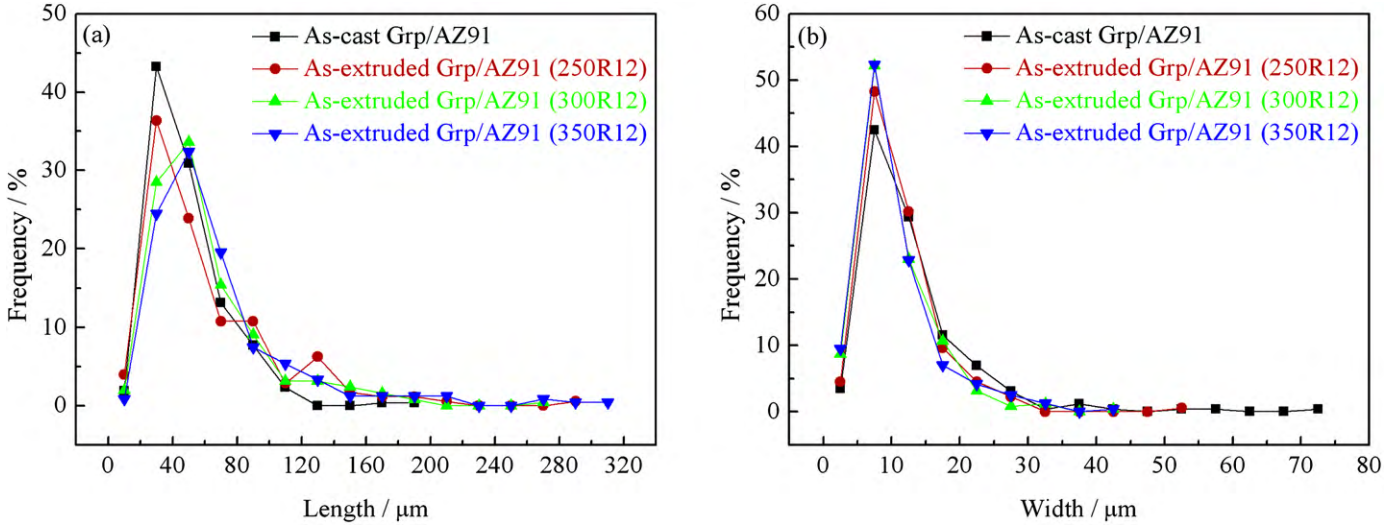

Fig. 4. Distribution of length and width of graphite particles before and after hot extrusion: (a) length; (b) width.

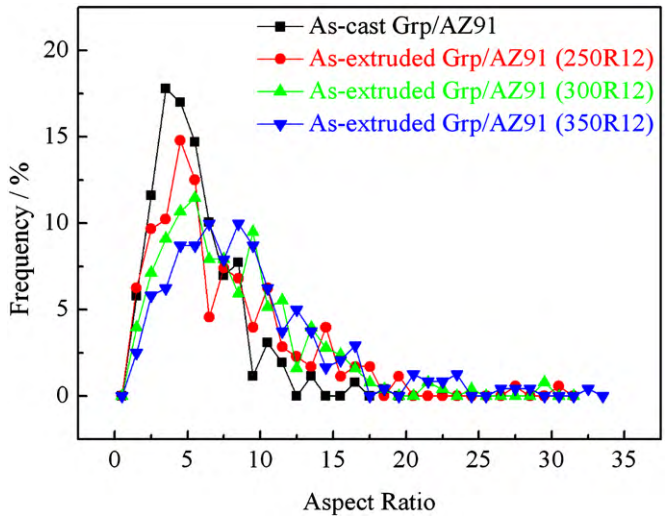

Fig. 5. Distribution of aspect ratio of graphite particles before and after hot extrusion.

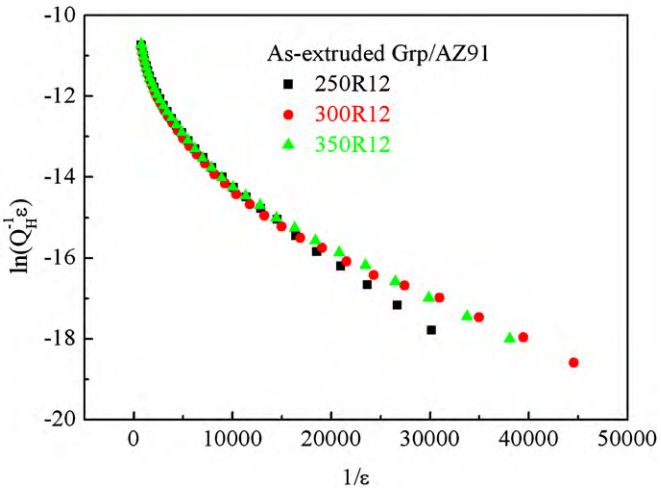

Fig. 7. G–L plots for as-extruded Grp/AZ91 composite at room temperature.

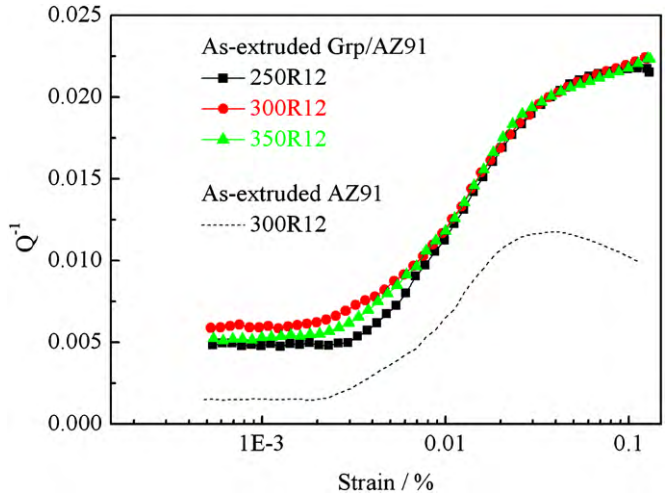

Fig. 6. Strain dependent damping capacities of as-extruded Grp/AZ91 composite and AZ91 alloy at room temperature with $f = 1$ Hz.

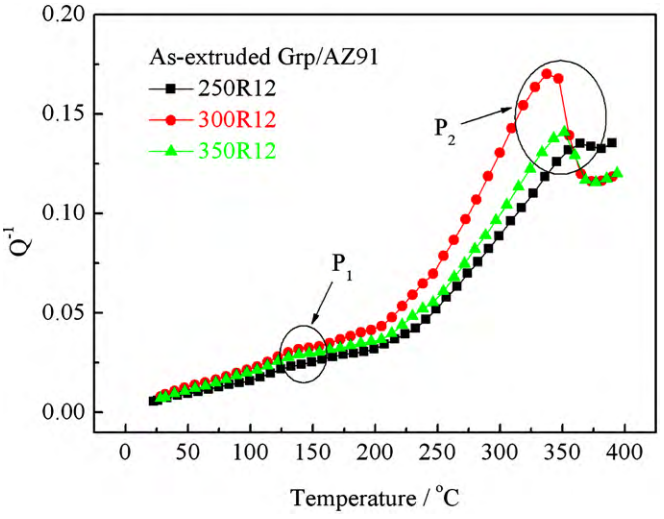

Fig. 8. Temperature dependent damping capacities of as-extruded Grp/AZ91 composite with $f = 1$ Hz, $\varepsilon = 4 \times 10^{-5}$ and $\dot{T} = 5\,^{\circ}$C/min.

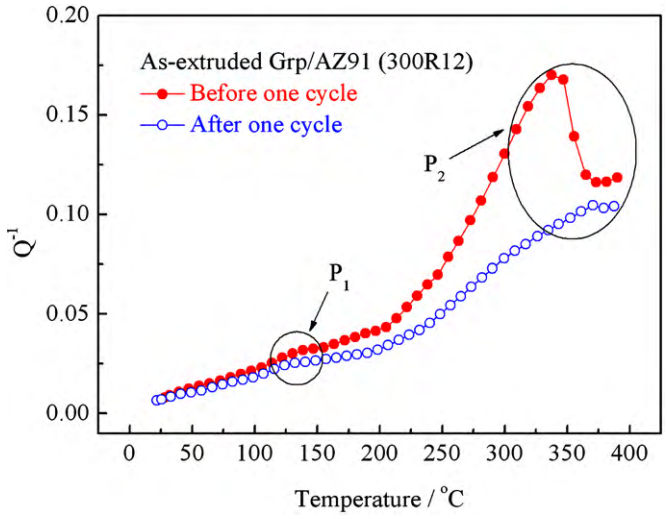

Fig. 9. Temperature dependent damping capacities of as-extruded Grp/AZ91 composite (300R12) before and after one temperature dependent damping test with $f = 1$ Hz, $\varepsilon = 4 \times 10^{-5}$ and $\dot{T} = 5\,^{\circ}$C/min.

testing temperature, and they rise with increasing temperature. Moreover, extrusion at 300 °C leads to the highest damping values at elevated temperatures when the strain is 4×10^{-5}. In addition, there are two definite damping peaks in the damping-temperature curves which occur at about 150 °C and 350 °C (marked as P_1 and P_2), respectively. The damping peak P_1 has no noticeable change with the increase of extrusion temperature, but damping peak P_2 changes significantly with the increase of extrusion temperature. The temperature dependent damping capacities of as-extruded Grp/AZ91 composite (300R12) before and after one temperature dependent damping test are displayed in Fig. 9. It is seen that the damping peak P_1 changes little after test, but the damping peak P_2 changes remarkably: the peak height decreases significantly, and the peak temperature shifts to higher temperature. Considering that little previous analytical and experimental work has been reported on such damping peaks, further information from other analyses is needed to clarify their origin.

Among the three extrusion temperatures, extrusion at 300 °C leads to the highest damping values in both damping-strain curves and damping-temperature curves, which can be attributed to the effect of particles/matrix interfaces and grain boundaries on damping capacities. Extrusion at 250 °C leads to the smallest grains and aspect ratio of graphite particles, i.e. the highest grain boundary damping and lowest particles/matrix interface damping. Extrusion at 350 °C leads to the biggest grains and aspect ratio of graphite particles, i.e. the lowest grain boundary damping and highest particles/matrix interface damping. On the other hand, extrusion at 300 °C leads to relatively small grains and relatively big aspect ratio of graphite particles, i.e. the composite extruded at 300 °C has relatively high grain boundary damping and particles/matrix interface damping simultaneously. Therefore, the composite extruded at 300 °C has the highest damping values due to the combined contribution of grain boundary damping and particles/matrix interface damping. Moreover, the improvement of damping capacities by the addition of graphite particles can be primarily attributed to the appearance of intrinsic damping of graphite particles and particles/matrix interface damping in the composite.

4. Conclusions

In the present work, the microstructures and damping capacities of as-extruded Grp/AZ91 magnesium matrix composite were investigated. The following results were obtained:

(1) Extrusion at 250 °C leads to the finest grains, and the aspect ratio of graphite particles increases as the extrusion temperature rises.
(2) In damping-strain curves, extrusion at 300 °C leads to the highest damping values in low strain region at room temperature. However, the damping values are very similar in relatively high strain region.
(3) In damping-temperature curves, extrusion at 300 °C leads to the highest damping values at elevated temperatures when the strain is 4×10^{-5}. In addition, there are two definite damping peaks which occur at about 150 °C and 350 °C, respectively.
(4) The damping capacities are improved significantly by the addition of graphite particles. Compared with AZ91 alloy extruded at 300 °C, the Q_0^{-1} of Grp/AZ91 composite is increased by nearly 400%.

References

[1] C.F. Zhang, T.X. Fan, W. Cao, D. Zhang, Mater. Sci. Eng. A 508 (2009) 190–194.
[2] W.G. Wang, C. Li, Y.L. Li, X.P. Wang, Q.F. Fang, Mater. Sci. Eng. A 518 (2009) 190–193.
[3] J. Hu, X.F. Wang, G.Y. Liu, Mater. Sci. Eng. A 527 (2010) 657–662.
[4] G. Liu, W.C. Ren, Y.L. Sun, J. Hu, Mater. Sci. Eng. A 527 (2010) 5136–5142.
[5] D.Q. Wan, J.C. Wang, G.F. Wang, G.C. Yang, Mater. Lett. 63 (2009) 391–393.
[6] D.Q. Wan, J.C. Wang, G.C. Yang, Mater. Sci. Eng. A 517 (2009) 114–117.
[7] Q. Miao, L.X. Hu, X. Wang, E.D. Wang, J. Alloys Compd. 493 (2010) 87–90.
[8] G.L. Ma, G. Han, X.F. Liu, J. Alloys Compd. 491 (2010) 165–169.
[9] S.F. Liu, Y. Zhang, H. Han, B. Li, J. Alloys Compd. 487 (2009) 202–205.
[10] K.N. Braszczyńska-Malik, J. Alloys Compd. 487 (2009) 263–268.
[11] B. Nami, S.G. Shabestari, S.M. Miresmaeili, H. Razavi, Sh. Mirdamadi, J. Alloys Compd. 489 (2010) 570–575.
[12] Y.W. Wu, K. Wu, K.K. Deng, K.B. Nie, X.J. Wang, M.Y. Zheng, X.S. Hu, Mater. Des. 31 (2010) 4862–4865.
[13] Q.Z. Wang, F.S. Han, C.X. Cui, J. Mater. Sci. 42 (2007) 5029–5035.
[14] T. Homma, N. Kunito, S. Kamado, Scr. Mater. 61 (2009) 644–647.
[15] X.M. Zhang, L. Li, Y.L. Deng, N. Zhou, J. Alloys Compd. 481 (2009) 296–300.
[16] K. Wu, K.K. Deng, K.B. Nie, Y.W. Wu, X.J. Wang, X.S. Hu, M.Y. Zheng, Mater. Des. 31 (2010) 3929–3932.
[17] K. Oh-Ishi, C.L. Mendis, T. Homma, S. Kamado, T. Ohkubo, K. Hono, Acta Mater. 57 (2009) 5593–5604.
[18] X.S. Hu, K. Wu, M.Y. Zheng, Scr. Mater. 54 (2006) 1639–1643.
[19] A. Granato, K. Lücke, J. Appl. Phys. 27 (1956) 583–593.
[20] A. Granato, K. Lücke, J. Appl. Phys. 27 (1956) 789–805.